



Particle Acceleration at Structure Formation Shocks

Hyesung Kang

Department of Earth Sciences, Pusan National University, Busan 46241, Republic of Korea

Abstract

Cosmological hydrodynamic simulations have demonstrated that shock waves could be produced in the intergalactic medium by supersonic flow motions during the course of hierarchical clustering of the large-scale-structure in the Universe. Similar to interplanetary shocks and supernova remnants (SNRs), these structure formation shocks can accelerate cosmic ray (CR) protons and electrons via diffusive shock acceleration. External accretion shocks, which form in the outermost surfaces of nonlinear structures, are as strong as SNR shocks and could be potential accelerations sites for high energy CR protons up to 10^{18} eV. But it could be difficult to detect their signatures due to extremely low kinetic energy flux associated with those accretion shocks. On the other hand, radiative features of internal shocks in the hot intracluster medium have been identified as temperature and density discontinuities in X-ray observations and diffuse radio emission from accelerated CR electrons. However, the non-detection of gamma-ray emission from galaxy clusters due to π^0 decay still remains to be an outstanding problem.

Keywords: acceleration of particles, cosmic rays, shock waves

1. Introduction

In [1] shocks in the intracluster medium (ICM) appeared as candidate acceleration sites for ultra-high-energy cosmic rays (CRs) in the so-called ‘Hillas diagram’, in which the maximum energy of CR nuclei achievable by a cosmic accelerator was estimated from the confinement condition:

$$E_{\max}(\text{ZeV}) \sim z \cdot \beta_a \cdot B_{\mu\text{G}} \cdot L_{\text{Mpc}}, \quad (1)$$

where E_{\max} is given in units of 10^{21} eV, z is the charge of CR nuclei, and $\beta_a = v_a/c$, $B_{\mu\text{G}}$, and L_{Mpc} are the characteristic speed, the magnetic field strength in units of microgauss, and the size in units of Mpc of the accelerator, respectively. For shocks associated with galaxy clusters with $\beta_a \sim 0.01$, $B_{\mu\text{G}} \sim 1$, $L_{\text{Mpc}} \sim 1$, CR protons could be accelerated up to $\sim 10^{19}$ eV.

[2] first suggested that cosmic shocks induced by the structure formation can accelerate CR protons up to

$10^{19.5}$ eV via diffusive shock acceleration (DSA). Independently and more or less simultaneously, [3] showed, using cosmological hydrodynamic simulations, that accretion shocks around galaxy clusters have $v_s \sim 3 \times 10^3$ km s $^{-1}$, and suggested that, for the Bohm diffusion with microgauss magnetic fields, the maximum energy of protons achieved via DSA by cluster accretion shocks is limited to ~ 60 EeV ($\tau_{\text{acc}} = \tau_{\text{pion}}$), due to the energy loss via photo-pion interactions with the cosmic background radiation (see Figure 1). Adopting simple models for magnetic field strength and DSA, and an analytic relation between the cluster temperature and the spherical accretion shock, [4] showed that the CR protons from a cosmological ensemble of cluster accretion shocks could make a significant contribution to the observed CR flux near 10^{19} eV.

Observational evidence for the electron acceleration by a cluster accretion shock was first suggested by [5] who proposed that diffuse radio relics detected in the outskirts of several clusters could be diffuse synchrotron emission from fossil electrons re-energized by

Email address: hskang@pusan.ac.kr (Hyesung Kang)

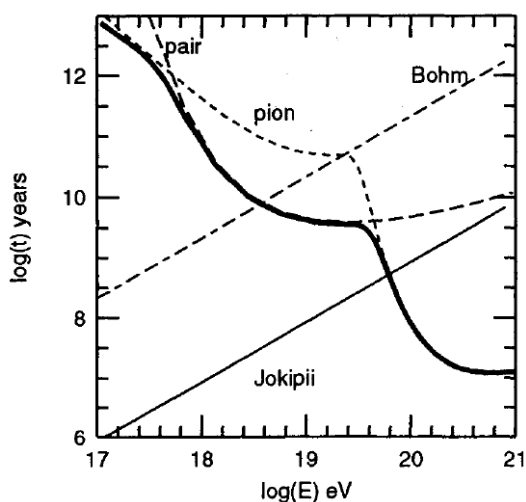


Figure 1: Energy loss time scales for CR protons due to pair-production (τ_{pair} , thick dashed line) and pion-production (τ_{pion} , thin dashed) on the cosmic background radiation. The thick solid line represents the time scale due to the sum of the two loss processes. Shock acceleration time scales for Bohm (τ_{Bohm} , dot-dashed) and Jokipii (τ_{Jokipii} , thin solid) diffusion at the shock with $u_s = 10^3 \text{ km s}^{-1}$ and $B = 1 \mu\text{G}$ [4].

accretion shocks. Since the discovery of a shock in the Bullet cluster (1E 0657-56) [6], about a dozen of shocks have been detected as sharp discontinuities in X-ray temperature or surface brightness in mainly merging clusters [7, 8]. Moreover, giant radio relics such as the Sausage relic in CIZA J2242.8+5301 and the Toothbrush relic in 1RXS J0603.3+4214 are thought to result from merger-driven shocks, since most of observed properties can be explained by synchrotron emission from shock-accelerated electrons cooling behind the shock [9, 10]. So the presence of cosmic shocks in the ICM within a few Mpc from the cluster center has been established, although shocks in lower density filaments await to be detected by future observational facilities [11, 12].

In this contribution, we review the properties of structure formation shocks, the physical processes involved in the acceleration of CR ions and electrons at collisionless shocks, and observational signatures of shocks and nonthermal particles in the ICM.

2. Properties of Structure Formation Shocks

The properties and energetics of cosmological shocks have been studied extensively, using numerical simulations for the large-scale-structure (LSS) formation [e.g., 13, 14, 15, 16, 17, 18]. The average spatial frequency

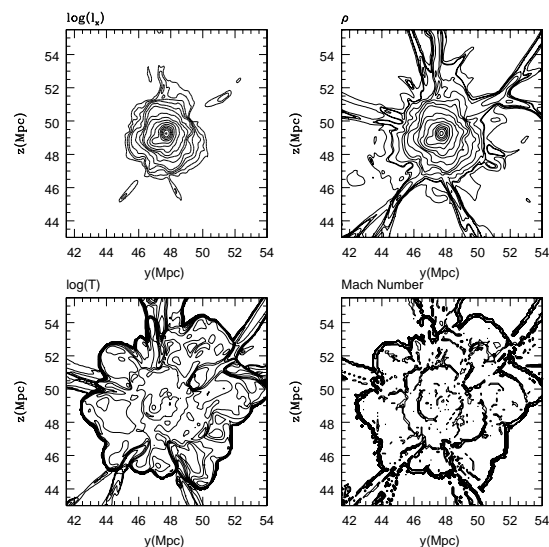


Figure 2: Two-dimensional slice showing X-ray emissivity, gas density, temperature, and shock locations around a galaxy cluster in a structure formation simulation. Strong external accretion shocks form in the outer surfaces of the cluster, while weak internal shocks reside inside the virialized central region [14].

between shock surfaces is $\sim 1 \text{ Mpc}^{-1}$ inside nonlinear structures of clusters, filaments, and sheets. These shocks can be classified mainly into two categories: (1) external accretion shocks with the Mach number, $3 \lesssim M_s \lesssim 100$, that form around the outermost surfaces of nonlinear structures, and (2) internal shocks mostly with $M_s \lesssim 5$ that form in the hot ICM inside nonlinear structures [14]. In Figure 2, external accretion shocks encompassing the cluster coincide with the region with sharp temperature discontinuities, indicating high Mach number shocks. On the other hand, weak internal shocks within a few Mpc from the cluster center are associated with mild temperature variations. The presence of internal shocks has been confirmed in many merging clusters, while radiative signature of external accretion shocks have not been detected so far due to very low surface brightness.

Weak internal shocks with $2 \lesssim M_s \lesssim 3$ have high kinetic energy flux and are responsible for most of the shock energy dissipation into heat and nonthermal components of the ICM such as CRs, magnetic fields, and turbulence. By adopting a DSA model of CR proton acceleration, [14] predicted that the ratio of the CR proton to gas thermal energies dissipated at all cosmological shocks through the history of the Universe could be substantial, perhaps up to 50%. However, this estimate has to be revised to significantly lower values as we will

discuss in Section 5.

3. Turbulence and Magnetic Fields in Large-Scale-Structure

Magnetic field is one of the key elements that govern the plasma processes at collisionless shocks and radiative signatures of accelerated particles. The intergalactic space is observed to be permeated with magnetic fields and filled with turbulence and CRs, similar to the interstellar medium within our Galaxy [15, 19, 20, 11, 12]. Analysis of the rotation measure data for Abell clusters indicates that the mean magnetic field strength ranges up to several μG in the ICM [21, 22].

Using hydrodynamic and magnetohydrodynamic (MHD) simulations for the structure formation, it has been suggested that turbulence could be produced in the ICM by cascade of the vorticity generated behind cosmological shocks or by merger-driven flow motions, and that the intergalactic magnetic fields could be amplified via turbulence dynamo [19, 23, 24, 25]. The seed fields might have been injected into the ICM via galactic winds and AGN jets or originate from some primordial processes [20, 11, 12]. This turbulence dynamo scenario typically predicts that the energy budget among different components in the ICM could be $E_{\text{turb}} \sim 0.1E_{\text{th}}$ and $E_B \sim 0.01E_{\text{th}}$, where E_{th} is the thermal energy density [19]. As shown in Figure 3, the volume-averaged magnetic field strength ranges $0.1 - 1 \mu\text{G}$ in the ICM ($T > 10^7 \text{ K}$) and $0.01 - 0.1 \mu\text{G}$ in filaments ($10^5 < T < 10^7 \text{ K}$), which seems to be consistent with observations [22, 21]. In the peripheral regions $\sim 5 \text{ Mpc}$ away from the cluster center where external accretions are expected to form, the magnetic field strength should be similar to that of filaments, i.e., $\sim 0.01 - 0.1 \mu\text{G}$. The magnetic fields should be much weaker in sheet-like structures and voids, but neither theoretical nor observational estimates are well defined in such low density regions.

Relativistic protons and electrons with the same rigidity ($R = pc/ze$) are accelerated in the same way in DSA regime. But for the particle injection to the DSA process, the obliquity angle, Θ_{Bn} , becomes an important factor. At quasi-parallel shocks ($\Theta_{\text{Bn}} \lesssim 45^\circ$), where the magnetic field direction is roughly parallel to the flow velocity, MHD waves are self-generated due to streaming of CR protons upstream of the shock, and protons are injected/accelerated efficiently to high energies via DSA [26, 27, 28]. At quasi-perpendicular shocks ($\Theta_{\text{Bn}} \gtrsim 45^\circ$), on the other hand, electrons tend to be reflected at the shock front and accelerated via shock drift acceleration (SDA) and may further go through the

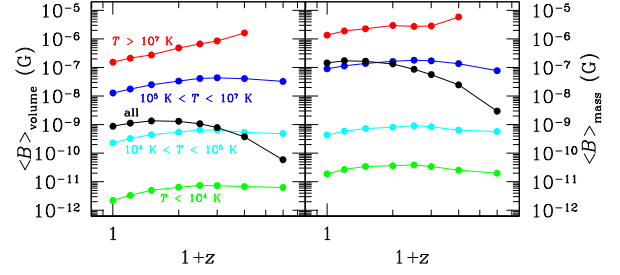


Figure 3: Magnetic field amplification based on turbulence dynamo in a structure formations simulation. Volume-averaged (left) and mass-averaged (right) magnetic field strength as a function of redshift z for the intergalactic medium in four temperature ranges, $T > 10^7 \text{ K}$ (red, ICM), $T = 10^5 - 10^7 \text{ K}$ (blue, WHIM), $T = 10^4 - 10^5 \text{ K}$ (cyan), and $T < 10^4 \text{ K}$ (green), and for all (black) the gas [19].

Fermi I acceleration process, if they are scattered by plasma waves excited in the preshock region [29].

In addition to Θ_{Bn} , excitation of MHD/kinetic waves by plasma instabilities and wave-particle interactions at collisionless shocks depend on the shock parameters such as the plasma beta, $\beta_p = P_{\text{gas}}/P_B$, and the Alfvén Mach number, $M_A \approx \sqrt{\beta_p} M_s$. For the internal ICM shocks, $\beta_p \sim 50$, $M_s \lesssim 3$, and $M_A \lesssim 20$. So they are super-critical, i.e., $M_A > M_{\text{crit}}$, where the critical Mach Number is $M_{\text{crit}} \sim 1 - 1.5$ for high beta plasma, and some ions are reflected specularly at the shock ramp, independent of the obliquity angle [30]. In the foreshock region, some of incoming ions and electrons are reflected upstream, and the drift between incoming and reflected particles may excite plasma waves via various micro-instabilities, depending on the shock parameters. For low beta plasma ($\beta_p \lesssim 1$), at high M_A quasi-perpendicular shocks ($M_A \gtrsim \sqrt{\beta_p m_p/m_e}/2$) the Buneman instability is known to excite electrostatic waves, leading to the shock-surfing-acceleration of electrons in the shock foot [31]. For low M_A quasi-perpendicular shocks ($M_A \lesssim \sqrt{m_p/m_e}/2$), on the other hand, the modified two stream instability could generate oblique whistler waves, which result in the pre-heating of thermal electrons to a κ -like suprathermal distribution [32].

4. Electron Acceleration at Cosmological Shocks

Plasma kinetic processes govern the preacceleration of electrons in the shock transition zone, which leads to the injection of CR electrons to the Fermi I process. Figure 4 shows thermal and suprathermal distributions of electrons and protons for the gas with $kT \approx 4.3 \text{ keV}$.

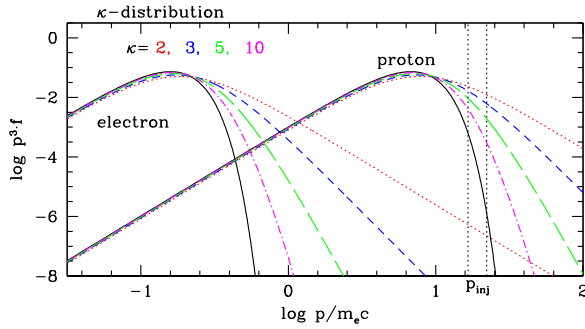


Figure 4: Momentum distribution, $p^3 f(p)$, of electrons and protons for the gas with $kT \approx 4.3$ keV in the case of the κ -distributions with $\kappa = 2, 3, 5,$ and 10 . The Maxwellian distributions are shown in black solid lines. The vertical lines indicate the range of the injection momentum of $p_{inj} = (3.5 - 4) p_{th,p}$ above which particles can be injected into the DSA process [33].

The particle momentum should be greater than a few times the postshock thermal proton momentum ($p_{th,p}$) to cross the shock transition. So thermal electrons with $p_{th,e} = p_{th,p} \sqrt{m_e/m_p}$ need to be pre-accelerated to the injection momentum, $p_{inj} \sim 3.5 p_{th,p}$, before they can start participating to the full DSA process [34]. Such injection from the thermal Maxwellian pool is expected to be very inefficient, especially at low Mach number shocks, and depend very sensitively on the shock Mach number. But if there are suprathermal electrons with the κ -like power-law tail, instead of the Maxwellian distribution, the injection and acceleration of electrons can be enhanced greatly even at weak cluster shocks [33]. As illustrated in Figure 4, the particle injection flux at p_{inj} is larger for a κ -distribution with a smaller value of κ . So the development of a κ -like suprathermal distribution is critical in the electron acceleration via DSA.

In the case of low M_A quasi-perpendicular shocks in the high beta ICM plasma, some incoming electrons are mirror reflected at the shock ramp and gain energy via multiple cycles of SDA, while protons can go through a few SDA cycles with only minimal energy gains [29]. In the foreshock of such weak shocks, the electron firehose instability induces oblique magnetic waves, which in turn provide efficient scattering necessary to energize the thermal electrons to suprathermal energies, leading to efficient injection to the DSA process. This picture is consistent with the observational fact that the magnetic field obliquity is typically quasi-perpendicular at giant radio relics such as the Sausage relic [9], and the double relic in the cluster PSZ1 G108.18 [35].

Radio relics are diffuse radio structures detected in the outskirts of merging galaxy clusters. Their observed

properties can be best understood by synchrotron emission from relativistic electrons accelerated at merger-driven shocks: elongated morphologies over ~ 2 Mpc, spectral aging across the relic width (behind the putative shock), integrated radio spectra of a power-law form with gradual steepening above ~ 2 GHz, and high polarization levels [9, 10, 11, 36].

The sonic Mach number of a relic shock can be estimated from either radio or X-ray observations, using the radio spectral index relation, $\alpha_{sh} = (M_{rad}^2 + 3)/2(M_{rad}^2 - 1)$, or the X-ray temperature jump condition, $T_2/T_1 = (M_X^2 + 3)(5M_X^2 - 1)/16/M_X^2$, respectively. In some radio relics, the two estimates are different, i.e., $M_X < M_{rad}$, indicating that the simple DSA origin of radio relics might not explain the observed properties [37]. For example, $M_X \approx 1.2 - 1.5$ and $M_{rad} \approx 3.0$ for the Toothbrush relic [38], while $M_X \approx 2.7$ and $M_{rad} \approx 4.6$ for the Sausage relic [9, 39]. Such discrepancy could be explained by the two following scenarios based on DSA: (1) injection-dominated model in which $M_s \approx M_{rad}$ and M_X is under-estimated due to projection effects in X-ray observation [40], and (2) reacceleration-dominated model in which preexisting electrons with a flat energy spectrum is reaccelerated by a weak shock with $M_s \approx M_X$ [41, 42]. Figure 5 illustrates that such two viable scenarios, albeit with different sets of model parameters, could reproduce the observed surface brightness and spectral index profiles of the Toothbrush relic [38].

Using structure formation simulations, [40] carried out mock observations of radio relic shocks detected in simulated clusters and showed that X-ray observations are inclined to detect weaker shocks due to projection effects, while radio observations tend to observe stronger shocks with flatter radio spectra. This naturally supports the injection-dominated model, in which M_X tends to be smaller than M_{rad} for a given radio relic.

The ICM is thought to contain fossil relativistic electrons left over from tails and lobes of extinct AGNs. Mildly relativistic electrons with $\gamma_e \lesssim 10^2$ survive for long periods of time, since the cooling time scale of electrons in $B \sim 1 \mu\text{G}$ is $t_{rad} \approx 10^{10} \text{ yr} \cdot (10^2/\gamma_e)$. They could provide seed electrons to the DSA process, which alleviates the low injection/acceleration efficiency problem at weak cluster shocks in the case of the injection-dominated model. If we conjecture that radio relics form when the ICM shocks encounter fossil mildly relativistic electrons with $\gamma_e \lesssim 10^2$, then the model may explain why only about 10 % of merging clusters contain radio relics [42].

The so-called infall shocks form in the cluster outskirts when the WHIM from adjacent filaments pene-

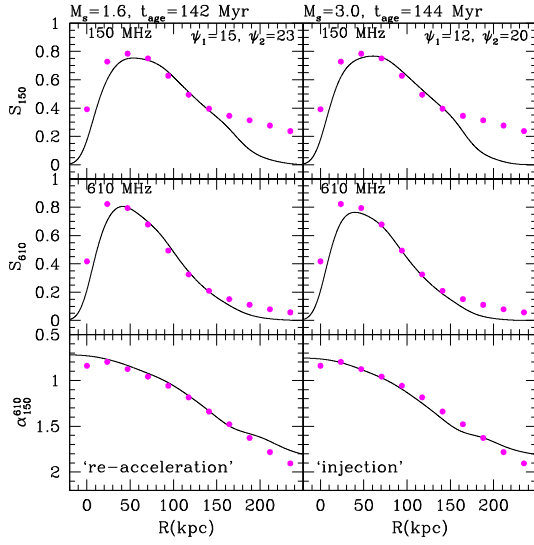


Figure 5: DSA modeling for the Toothbrush relic: reacceleration-dominated model with a $M_s \approx 1.6$ shock (left panels) and injection-dominated model with a $M_s = 3.0$ shock (right panels). Radio flux density S_ν at 150 MHz (top) and at 610 MHz (middle), and the spectral index α_{150}^{610} between the two frequencies (bottom) are plotted as a function of the projected distance behind the shock (relic edge), $R(\text{kpc})$ [42]. The magenta dots are the observational data of the head portion of the Toothbrush relic [38].

trates deeply into the ICM [43]. They have relatively high Mach numbers ($M_s \gtrsim 3$) and large kinetic energy fluxes, so they could contribute to a significant fraction of CR production in clusters with actively infalling filaments. So some radio relics with relatively flat radio spectra found in the cluster outskirts could be explained by these energetic infall shocks.

Although there still remain a few puzzles regarding the DSA origin of radio relics, it is well received that shocks should be induced in merging galaxy clusters and radio relics could be radiative signatures of relativistic electrons accelerated at those shocks [11, 12].

5. Proton Acceleration at Cosmological Shocks

In the precursor of quasi-parallel shocks, CR protons streaming ahead of the shock are known to excite both resonant and non-resonant waves and amplify the turbulent magnetic fields by orders of magnitude [44, 26]. According to hybrid simulations by [27], the CR proton acceleration is efficient only for quasi-parallel shocks with $\Theta_{\text{Bn}} \lesssim 45^\circ$, and about 6 – 10% of the postshock energy is transferred to CR proton energy for shocks with $M_A \sim 5 - 10$. For quasi-perpendicular shocks,

on the other hand, protons go through only a few cycles of SDA before they advect downstream away from the shock. So scattering waves are not self-generated in the preshock region, and thus the CR proton acceleration is very inefficient. Note that for these simulations, $\beta_p \sim 1$ and $M_A \sim M_s$, so the quantitative estimates for the CR acceleration efficiency may be different for the ICM shocks in high beta plasmas. Based on cosmological simulations with magnetic fields, the shock obliquity angle is expected to have the random orientation in the ICM and at surrounding accretions shocks [19]. Then the probability distribution function for the obliquity angle scales as $P(\Theta_{\text{Bn}}) \propto \sin \Theta_{\text{Bn}}$, so only $\sim 30\%$ of all cosmological shocks have the quasi-parallel configuration and accelerate CR protons [45].

Using cosmological hydrodynamic simulations, the γ -ray emission from galaxy clusters have been estimated by modeling the production of CR protons and electrons at structure formation shocks in several studies [e.g., 46, 47, 48, 45]. Inelastic collisions of shock-accelerated protons with thermal protons produce neutral pions, which decay into γ -ray photons (hadronic origin) [46]. Inverse Compton upscattering of the cosmic background radiation by shock-accelerated primary CR electrons and by secondary CR electrons generated by decay of charged pions also provides γ -ray emission (leptonic origin) [49]. It has been shown that the hadronic γ -ray emission is expected to dominate over the leptonic contribution in the central ICM within the virial radius [e.g., 48].

The key parameters in predicting the π^0 decay γ -ray emission are the CR proton acceleration efficiency, $\eta(M_s)$, defined as the ratio of the CR energy flux to the shock kinetic energy flux, and the volume-averaged ratio of the CR to thermal pressure in the ICM, $\langle X_{\text{CR}} \rangle = \langle P_{\text{CR}} \rangle / \langle P_{\text{th}} \rangle$ [15, 50, 48]. Adopting the DSA efficiency model in which $\eta \approx 0.1$ for $M_s \approx 3$ given in [51], for example, [48] estimated that $\langle X_{\text{CR}} \rangle \approx 0.02$ for Coma-like clusters. In [50], in which a thermal-leakage injection model was implemented to DSA simulations, the efficiency is estimated to be $\eta \approx 0.01 - 0.1$ for $M_s \approx 3 - 5$ shocks. Note that in this DSA model the efficiency depends sensitively on the assumed injection model as well as M_s .

Recently, [45] tested several different prescriptions for the DSA efficiency by comparing the γ -ray flux from simulated clusters with the Fermi-LAT upper-limit flux levels of observed clusters. Even with the relatively less efficient model based on the hybrid simulation results of [27], in which $\eta \approx 0.05$ for $M_A = 5$ quasi-parallel shocks, and the consideration of the random magnetic field directions, they find that about 10-20 % of simu-

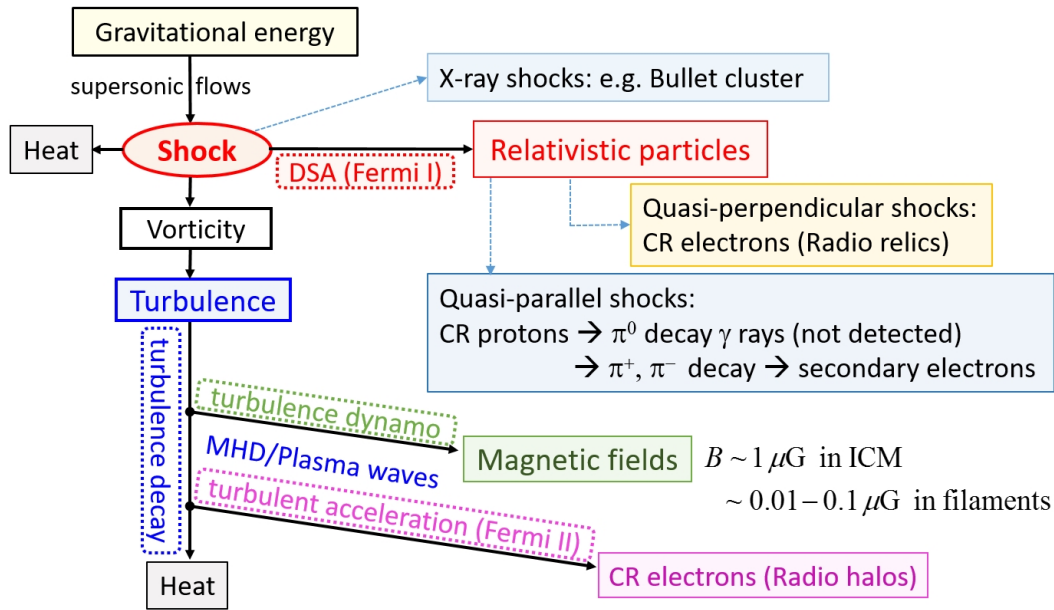


Figure 6: Physical processes and observational signatures expected to operate at structure formation shocks

lated clusters have the predicted γ -ray flux levels above the Fermi-LAT upper limits. So the authors suggested that only if $\eta \leq 10^{-3}$ for all Mach number shocks, which results in the average value of $\langle X_{\text{CR}} \rangle \lesssim 0.01$ in the ICM, the predicted γ -ray fluxes from simulated clusters can stay below the Fermi-LAT upper limits. This agrees with the conclusion of [52], which predicted $\langle X_{\text{CR}} \rangle \lesssim 0.0125 - 0.014$ based on the analysis of four year Fermi-LAT data.

Non-detection of γ -ray emission from galaxy clusters might be explained, if the CR proton acceleration is much less efficient than expected in the current DSA theory (i.e. $\eta \lesssim 10^{-3}$ for $M_s \sim 3$). In that regard, the proton acceleration at weak shocks in the low density, high beta ICM plasma needs to be investigated further, since so far most of hybrid/PIC plasma simulations have focused on strong shocks in $\beta_p \lesssim 1$ ISM and solar wind plasma.

Finally, armed with our new understandings based on the recent plasma hybrid simulations [27, 28], it is worth examining if strong accretions shock can accelerate CR protons to ultra-high energies. The protons are expected to be accelerated efficiently via DSA only in the quasi-parallel portion of the outermost surfaces encompassed with accretion shocks. There magnetic fields could be amplified via Bell's non-resonant hybrid instability by a factor of $B/B_0 \propto \sqrt{M_A}$ [28], where $B_0 \sim 0.01\mu\text{G}$ and $M_A \sim 300$. So it is reasonable to assume the magnetic field strength at external accretion shocks is $B \sim 0.1\mu\text{G}$,

about one order of magnitude smaller than that typically adopted in the previous studies [e.g., 2, 3]. Considering the photo-pair energy losses, protons can be accelerated up to $E_{p,\text{max}} \sim 10^{18}$ eV at quasi-parallel accretion shocks (see Figure 1).

6. Summary

1. Astrophysical plasmas consist of both thermal and CR particles that are closely coupled with permeating magnetic fields and underlying turbulent flows. So understanding the complex network of physical interactions among these components, especially in the high beta collisionless ICM plasma, is crucial to the study of the particle acceleration at structure formation shocks (see Figure 6).
2. Gravitational energy associated with hierarchical clustering of the large-scale-structures must be dissipated at structure formation shocks into several different forms: heat, CRs, turbulence and magnetic fields [14].
3. The vorticity generated by curved shocks decays into turbulence behind the shock, which in turn cascades into MHD/plasma waves in a wide range of scales and amplify magnetic field via turbulence dynamo [19].
4. There is growing observational evidence indicating the presence of weak shocks, relativistic electrons,

microgauss level magnetic fields, and turbulence in the ICM of galaxy clusters [12].

5. CR protons are expected to be accelerated mainly at quasi-parallel shocks. For weak internal shocks ($M_s \lesssim 3$) with high kinetic energy fluxes that form in the ICM, the CR proton acceleration efficiency is likely to be $\eta < 0.01$ in order to explain the non-detection of γ -ray emission from galaxy clusters due to inelastic p - p collisions in the ICM [45].
6. At quasi-parallel portion of strong external accretion shocks, CR protons could be accelerated to $\sim 10^{18}$ eV, if the preshock magnetic fields can be amplified to $\sim 0.1\mu\text{G}$ via CR streaming instabilities [3, 27].
7. CR electrons are expected to be accelerated preferentially at quasi-perpendicular shocks [29]. Radio relics detected in the outskirts of merging clusters seem to reveal radiative signatures of relativistic electrons accelerated at merger-driven shocks mostly with $M_s \sim 2 - 3$ [41].
8. The injection of protons and electrons from thermal or suprathermal populations to the DSA process at collisionless shocks involves plasma kinetic processes such as excitation of waves by micro-instabilities as well as shock drift acceleration and shock surfing acceleration [33]. During the last decade significant progress been made in that front through PIC/hybrid plasma simulations of non-relativistic shocks [27, 29].

7. Acknowledgements

This work was supported by the National Research Foundation of Korea through grants NRF-2014R1A1A2057940 and NRF-2016R1A5A1013277. The author would like to thank D. Ryu for helpful comments on the paper.

References

- [1] A. M. Hillas, The Origin of Ultra-High-Energy Cosmic Rays, *ARA&A*22 (1984) 425–444. doi:10.1146/annurev.aa.22.090184.002233.
- [2] C. A. Norman, D. B. Melrose, A. Achterberg, The Origin of Cosmic Rays above 10 18.5 eV, *ApJ*454 (1995) 60. doi:10.1086/176465.
- [3] H. Kang, D. Ryu, T. W. Jones, Cluster Accretion Shocks as Possible Acceleration Sites for Ultra-High-Energy Protons below the Greisen Cutoff, *ApJ*456 (1996) 422. arXiv:astro-ph/9507113, doi:10.1086/176666.
- [4] H. Kang, J. P. Rachen, P. L. Biermann, Contributions to the Cosmic Ray Flux above the Ankle: Clusters of Galaxies, *MNRAS*286 (1997) 257–267. arXiv:astro-ph/9608071, doi:10.1093/mnras/286.2.257.
- [5] T. A. Ensslin, P. L. Biermann, U. Klein, S. Kohle, Cluster radio relics as a tracer of shock waves of the large-scale structure formation, *A&A*332 (1998) 395–409. arXiv:astro-ph/9712293.
- [6] M. Markevitch, A. H. Gonzalez, L. David, A. Vikhlinin, S. Murray, W. Forman, C. Jones, W. Tucker, A Textbook Example of a Bow Shock in the Merging Galaxy Cluster 1E 0657-56, *ApJ*567 (2002) L27–L31. arXiv:astro-ph/0110468, doi:10.1086/339619.
- [7] M. Markevitch, A. Vikhlinin, Shocks and cold fronts in galaxy clusters, *Phys. Rep.*443 (2007) 1–53. arXiv:astro-ph/0701821, doi:10.1016/j.physrep.2007.01.001.
- [8] H. R. Russell, J. S. Sanders, A. C. Fabian, S. A. Baum, M. Donahue, A. C. Edge, B. R. McNamara, C. P. O’Dea, Chandra observation of two shock fronts in the merging galaxy cluster Abell 2146, *MNRAS*406 (2010) 1721–1733. arXiv:1004.1559, doi:10.1111/j.1365-2966.2010.16822.x.
- [9] R. J. van Weeren, H. J. A. Röttgering, M. Brüggen, M. Hoeft, Particle Acceleration on Megaparsec Scales in a Merging Galaxy Cluster, *Science* 330 (2010) 347–. arXiv:1010.4306, doi:10.1126/science.1194293.
- [10] R. J. van Weeren, H. J. A. Röttgering, H. T. Intema, L. Rudnick, M. Brüggen, M. Hoeft, J. B. R. Oonk, The “toothbrush-relic”: evidence for a coherent linear 2-Mpc scale shock wave in a massive merging galaxy cluster?, *A&A*546 (2012) A124. arXiv:1209.2196, doi:10.1051/0004-6361/201219000.
- [11] M. Brüggen, A. Bykov, D. Ryu, H. Röttgering, Magnetic Fields, Relativistic Particles, and Shock Waves in Cluster Outskirts, *Space Sci. Rev.*166 (2012) 187–213. arXiv:1107.5223, doi:10.1007/s11214-011-9785-9.
- [12] G. Brunetti, T. W. Jones, Cosmic Rays in Galaxy Clusters and Their Nonthermal Emission, *International Journal of Modern Physics D* 23 (2014) 1430007–98. arXiv:1401.7519, doi:10.1142/S0218271814300079.
- [13] F. Miniati, D. Ryu, H. Kang, T. W. Jones, R. Cen, J. P. Ostriker, Properties of Cosmic Shock Waves in Large-Scale Structure Formation, *ApJ*542 (2000) 608–621. arXiv:astro-ph/0005444, doi:10.1086/317027.
- [14] D. Ryu, H. Kang, E. Hallman, T. W. Jones, Cosmological Shock Waves and Their Role in the Large-Scale Structure of the Universe, *ApJ*593 (2003) 599–610. arXiv:astro-ph/0305164, doi:10.1086/376723.
- [15] H. Kang, D. Ryu, R. Cen, J. P. Ostriker, Cosmological Shock Waves in the Large-Scale Structure of the Universe: Nongravitational Effects, *ApJ*669 (2007) 729–740. arXiv:0704.1521, doi:10.1086/521717.
- [16] S. W. Skillman, B. W. O’Shea, E. J. Hallman, J. O. Burns, M. L. Norman, Cosmological Shocks in Adaptive Mesh Refinement Simulations and the Acceleration of Cosmic Rays, *ApJ*689 (2008) 1063–1077. arXiv:0806.1522, doi:10.1086/592496.
- [17] M. Hoeft, M. Brüggen, G. Yepes, S. Gottlöber, A. Schwabe, Diffuse radio emission from clusters in the MareNostrum Universe simulation, *MNRAS*391 (2008) 1511–1526. arXiv:0807.1266, doi:10.1111/j.1365-2966.2008.13955.x.
- [18] F. Vazza, G. Brunetti, C. Gheller, Shock waves in Eulerian cosmological simulations: main properties and acceleration of cosmic rays, *MNRAS*395 (2009) 1333–1354. arXiv:0808.0609, doi:10.1111/j.1365-2966.2009.14691.x.
- [19] D. Ryu, H. Kang, J. Cho, S. Das, Turbulence and Magnetic Fields in the Large-Scale Structure of the Universe, *Science* 320 (2008) 909–. arXiv:0805.2466, doi:10.1126/science.1154923.
- [20] K. Dolag, A. M. Bykov, A. Diaferio, Non-Thermal Processes in Cosmological Simulations, *Space Sci. Rev.*134 (2008) 311–335.

- arXiv:0801.1048, doi:10.1007/s11214-008-9319-2.
- [21] T. E. Clarke, P. P. Kronberg, H. Böhringer, A New Radio-X-Ray Probe of Galaxy Cluster Magnetic Fields, *ApJ*547 (2001) L111–L114.
- [22] C. L. Carilli, G. B. Taylor, Cluster Magnetic Fields, *ARA&A*40 (2002) 319–348.
- [23] F. Vazza, G. Brunetti, A. Kritsuk, R. Wagner, C. Gheller, M. Norman, Turbulent motions and shocks waves in galaxy clusters simulated with adaptive mesh refinement, *A&A*504 (2009) 33–43. arXiv:0905.3169, doi:10.1051/0004-6361/200912535.
- [24] J. Cho, Origin of Magnetic Field in the Intracluster Medium: Primordial or Astrophysical?, *ApJ*797 (2014) 133. arXiv:1410.1893, doi:10.1088/0004-637X/797/2/133.
- [25] A. Beresnyak, F. Miniati, Turbulent Amplification and Structure of the Intracluster Magnetic Field, *ApJ*817 (2016) 127. arXiv:1507.00342, doi:10.3847/0004-637X/817/2/127.
- [26] A. R. Bell, Turbulent amplification of magnetic field and diffusive shock acceleration of cosmic rays, *MNRAS*353 (2004) 550–558. doi:10.1111/j.1365-2966.2004.08097.x.
- [27] D. Caprioli, A. Spitkovsky, Simulations of Ion Acceleration at Non-relativistic Shocks. I. Acceleration Efficiency, *ApJ*783 (2014) 91. arXiv:1310.2943, doi:10.1088/0004-637X/783/2/91.
- [28] D. Caprioli, A. Spitkovsky, Simulations of Ion Acceleration at Non-relativistic Shocks. II. Magnetic Field Amplification, *ApJ*794 (2014) 46. arXiv:1401.7679, doi:10.1088/0004-637X/794/1/46.
- [29] X. Guo, L. Sironi, R. Narayan, Non-Thermal Electron Acceleration in Low Mach Number Collisionless Shocks. II. Firehose-Mediated Fermi Acceleration and its Dependence on Pre-Shock Conditions, *ArXiv e-prints* arXiv:1409.7393.
- [30] R. A. Treumann, Fundamentals of collisionless shocks for astrophysical application, I. Non-relativistic shocks, *A&A Rev.*17 (2009) 409–535. doi:10.1007/s00159-009-0024-2.
- [31] T. Amano, M. Hoshino, Electron Shock Surfing Acceleration in Multidimensions: Two-Dimensional Particle-in-Cell Simulation of Collisionless Perpendicular Shock, *ApJ*690 (2009) 244–251. arXiv:0805.1098, doi:10.1088/0004-637X/690/1/244.
- [32] S. Matsukiyo, M. Scholer, Modified two-stream instability in the foot of high Mach number quasi-perpendicular shocks, *Journal of Geophysical Research (Space Physics)* 108 (2003) 1459. doi:10.1029/2003JA010080.
- [33] H. Kang, V. Petrosian, D. Ryu, T. W. Jones, Injection of κ -like Suprathermal Particles into Diffusive Shock Acceleration, *ApJ*788 (2014) 142. arXiv:1405.0557, doi:10.1088/0004-637X/788/2/142.
- [34] M. A. Malkov, L. O. Drury, Nonlinear theory of diffusive acceleration of particles by shock waves, *Reports on Progress in Physics* 64 (2001) 429–481. doi:10.1088/0034-4885/64/4/201.
- [35] F. de Gasperin, H. T. Intema, R. J. van Weeren, W. A. Dawson, N. Golovich, D. Wittman, A. Bonafede, M. Brüggen, A powerful double radio relic system discovered in PSZ1 G108.18-11.53: evidence for a shock with non-uniform Mach number?, *MNRAS*453 (2015) 3483–3498. arXiv:1508.02901, doi:10.1093/mnras/stv1873.
- [36] L. Feretti, G. Giovannini, F. Govoni, M. Murgia, Clusters of galaxies: observational properties of the diffuse radio emission, *A&A Rev.*20 (2012) 54. arXiv:1205.1919, doi:10.1007/s00159-012-0054-z.
- [37] H. Akamatsu, H. Kawahara, Systematic X-Ray Analysis of Radio Relic Clusters with Suzaku, *PASJ*65 (2013) 16. arXiv:1112.3030, doi:10.1093/pasj/65.1.16.
- [38] R. J. van Weeren et al., LOFAR, VLA, and Chandra Observations of the Toothbrush Galaxy Cluster, *ApJ*818 (2016) 204. arXiv:1601.06029, doi:10.3847/0004-637X/818/2/204.
- [39] H. Akamatsu, R. J. van Weeren, G. A. Ogrean, H. Kawahara, A. Stroe, D. Sobral, M. Hoeft, H. Röttgering, M. Brüggen, J. S. Kaastra, Suzaku X-ray study of the double radio relic galaxy cluster CIZA J2242.8+5301, *A&A*582 (2015) A87. arXiv:1507.02285, doi:10.1051/0004-6361/201425209.
- [40] S. E. Hong, H. Kang, D. Ryu, Radio and X-Ray Shocks in Clusters of Galaxies, *ApJ*812 (2015) 49. arXiv:1504.03102, doi:10.1088/0004-637X/812/1/49.
- [41] H. Kang, D. Ryu, T. W. Jones, Diffusive Shock Acceleration Simulations of Radio Relics, *ApJ*756 (2012) 97. arXiv:1205.1895, doi:10.1088/0004-637X/756/1/97.
- [42] H. Kang, Re-Acceleration Model for the “Toothbrush” Radio Relic, *Journal of Korean Astronomical Society* 49 (2016) 83–92. arXiv:1603.07444, doi:10.5303/JKAS.2016.49.3.83.
- [43] S. E. Hong, D. Ryu, H. Kang, R. Cen, Shock Waves and Cosmic Ray Acceleration in the Outskirts of Galaxy Clusters, *ApJ*785 (2014) 133. arXiv:1403.1420, doi:10.1088/0004-637X/785/2/133.
- [44] S. G. Lucek, A. R. Bell, Non-linear amplification of a magnetic field driven by cosmic ray streaming, *MNRAS*314 (2000) 65–74. doi:10.1046/j.1365-8711.2000.03363.x.
- [45] F. Vazza, M. Brüggen, D. Wittor, C. Gheller, D. Eckert, M. Stubbe, Constraining the efficiency of cosmic ray acceleration by cluster shocks, *MNRAS*459 (2016) 70–83. arXiv:1603.02688, doi:10.1093/mnras/stw584.
- [46] F. Miniati, D. Ryu, H. Kang, T. W. Jones, Cosmic-Ray Protons Accelerated at Cosmological Shocks and Their Impact on Groups and Clusters of Galaxies, *ApJ*559 (2001) 59–69. arXiv:astro-ph/0105465, doi:10.1086/322375.
- [47] C. Pfrommer, T. A. Enßlin, V. Springel, M. Jubelgas, K. Dolag, Simulating cosmic rays in clusters of galaxies - I. Effects on the Sunyaev-Zel’dovich effect and the X-ray emission, *MNRAS*378 (2007) 385–408. arXiv:astro-ph/0611037, doi:10.1111/j.1365-2966.2007.11732.x.
- [48] A. Pinzke, C. Pfrommer, Simulating the γ -ray emission from galaxy clusters: a universal cosmic ray spectrum and spatial distribution, *MNRAS*409 (2010) 449–480. arXiv:1001.5023, doi:10.1111/j.1365-2966.2010.17328.x.
- [49] F. Miniati, T. W. Jones, H. Kang, D. Ryu, Cosmic-Ray Electrons in Groups and Clusters of Galaxies: Primary and Secondary Populations from a Numerical Cosmological Simulation, *ApJ*562 (2001) 233–253. arXiv:astro-ph/0108305, doi:10.1086/323434.
- [50] H. Kang, D. Ryu, Diffusive Shock Acceleration at Cosmological Shock Waves, *ApJ*764 (2013) 95. arXiv:1212.3246, doi:10.1088/0004-637X/764/1/95.
- [51] T. A. Enßlin, C. Pfrommer, V. Springel, M. Jubelgas, Cosmic ray physics in calculations of cosmological structure formation, *A&A*473 (2007) 41–57. arXiv:astro-ph/0603484, doi:10.1051/0004-6361:20065294.
- [52] M. Ackermann et al., Search for Cosmic-Ray-induced Gamma-Ray Emission in Galaxy Clusters, *ApJ*787 (2014) 18. arXiv:1308.5654, doi:10.1088/0004-637X/787/1/18.